

Dosimetry and efficiency comparison of knowledge-based and manual planning using volumetric modulated arc therapy for craniospinal irradiation

Wei-Ta Tsai^{1,2}, Hui-Ling Hsieh², Shih-Kai Hung^{2,3}, Chi-Fu Zeng², Ming-Fen Lee², Po-Hao Lin², Chia-Yi Lin², Wei-Chih Li⁴, Wen-Yen Chiou^{2,3}, Tung-Hsin Wu¹

¹ Department of Biomedical Imaging and Radiological Sciences, National Yang Ming Chiao Tung University, Taipei, Taiwan

² Department of Radiation Oncology, Dalin Tzu Chi Hospital, Buddhist Tzu Chi Medical Foundation, Chiayi, Taiwan

³ School of Medicine, Tzu Chi University, Hualien, Taiwan

⁴ Departments of Radiation Oncology, Taichung Tzu Chi Hospital, Buddhist Tzu Chi Medical Foundation, Taichung, Taiwan

Radiol Oncol 2024; 58(2): 289-299.

Received 4 November 2023

Accepted 3 January 2024

Correspondence to: Tung-Hsin Wu, Ph.D., Department of Biomedical Imaging and Radiological Sciences, National Yang Ming Chiao Tung University, No. 155, Sec. 2, Linong St., Beitou Dist., Taipei City 112304, Taiwan, E-mail: tung@ym.edu.tw; Tel: (886) 02-28201095 and Wen-Yen Chiou, MD, Ph.D., Department of Radiation Oncology, Dalin Tzu Chi Hospital, Buddhist Tzu Chi Medical Foundation, No. 2, Ming Sheng Road, Dalin Town, Chiayi, 622401, Taiwan, E-mail: cwyuncu@gmail.com; Tel: (886) 05-2648000 extension 5695.

Disclosure: No potential conflicts of interest were disclosed.

This is an open access article distributed under the terms of the CC-BY license (<https://creativecommons.org/licenses/by/4.0/>).

Background. Craniospinal irradiation (CSI) poses a challenge to treatment planning due to the large target, field junction, and multiple organs at risk (OARs) involved. The aim of this study was to evaluate the performance of knowledge-based planning (KBP) in CSI by comparing original manual plans (MP), KBP RapidPlan initial plans (RP_i), and KBP RapidPlan final plans (RP_f), which received further re-optimization to meet the dose constraints.

Patients and methods. Dose distributions in the target were evaluated in terms of coverage, mean dose, conformity index (CI), and homogeneity index (HI). The dosimetric results of OARs, planning time, and monitor unit (MU) were evaluated.

Results. All MP and RP_f plans met the plan goals, and 89.36% of RP_i plans met the plan goals. The Wilcoxon tests showed comparable target coverage, CI, and HI for the MP and RP_f groups; however, worst plan quality was demonstrated in the RP_i plans than in MP and RP_f. For the OARs, RP_f and RP_i groups had better dosimetric results than the MP group ($P < 0.05$ for optic nerves, eyes, parotid glands, and heart). The planning time was significantly reduced by the KBP from an average of 677.80 min in MP to 227.66 min ($P < 0.05$) and 307.76 min ($P < 0.05$) in RP_i and RP_f, respectively. MU was not significantly different between these three groups.

Conclusions. The KBP can significantly reduce planning time in CSI. Manual re-optimization after the initial KBP is recommended to enhance the plan quality.

Key words: knowledge-based planning; RapidPlan; craniospinal irradiation; volumetric modulated arc therapy

Introduction

Prophylactic or therapeutic craniospinal irradiation (CSI) is an option for managing certain primary brain tumors, such as medulloblastoma, or hematologic malignancies.¹ Since the maximum

field of the linear accelerator is 40 cm by 40 cm, the conventional three-dimensional conformal radiation therapy (3D-CRT) techniques for CSI use two opposed lateral craniocervical fields adjoined by two adjacent posterior spinal fields. In conventional CSI techniques, the fields are matched between

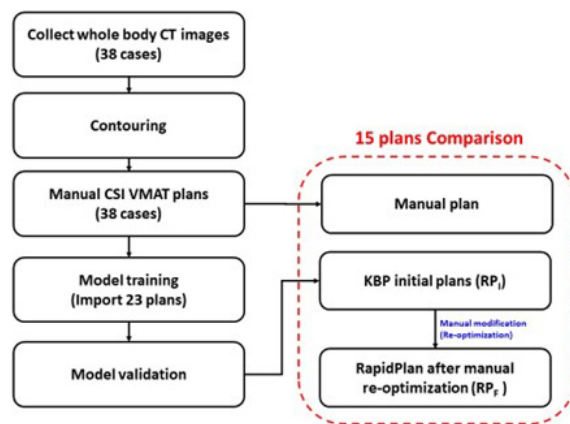


FIGURE 1. Flowchart of the study design.

CSI = craniospinal irradiation; CT = computed tomography; KBP = knowledge-based planning; VMAT = volumetric modulated arc therapy

the lateral and posterior fields, creating over- or underdosage within the spinal cord. To address this issue, 3D-CRT with the moving junction technique^{2,3}, which involves changing different junction locations daily during the treatment course, is an option to blur the dose ununiform effect.

The moving junction technique in 3D-CRT requires the use of multiple treatment plans, which increases the complexity of treatment planning and daily treatment. Moreover, the CSI moving junction technique can only reduce the dose ununiform effect but cannot obtain dose homogeneity as a common treatment. With the development of commercial treatment planning system (TPS), volumetric modulated arc therapy (VMAT) with multi-isocenter optimization⁴ was introduced. VMAT with 360-degree beams can achieve higher conformity and better dispersion of normal organs compared to conventional 3D-CRT.^{5,6} The VMAT technique with large field overlaps for low-dose gradient junction could tolerate greater positional shifts while maintaining homogeneous dose.^{7,8} However, planning CSI using the high-precision VMAT technique is challenging and time-consuming for medical physicists due to the long treatment field from the brain to the lumbosacral region, which significantly exceeds the treatment field size of a linear accelerator and involves more than ten organs at risk. Because CSI treatment is relatively rare and only patients with possible malignancy tumor cells seeding in the craniospinal canal receive this treatment, medical physicists in many institutions are unfamiliar with this technique. The rarity of the expertise and complex planning processes make this process resource-intensive.

Knowledge-based planning (KBP) is based on a model of estimating dose-volume histograms (DVHs), which is configured by a library of historical treatment plans with the aim of improving planning efficiency.⁹ In previous studies, KBP has been adopted to treat patients with several cancer types, such as head and neck cancers and pelvic malignancies.¹⁰⁻¹³ KBP showed improved planning efficiency with well-reserved plan quality in those cancer sites. However, compared to those cancer sites, CSI would require more treatment isocenters and patients moving with junction feathering. Moreover, more organs at risk (OARs) needed to be considered in CSI than other treatment sites. Reviewing the literature, previous CSI studies have not compared the plan quality and cost-effectiveness of the general manual plan method and the KBP with and without re-optimization.

This study aimed to compare the plan quality and efficiency of the original manual plans (MP), KBP initial plans (RP_i) (RapidPlan™, Varian Medical Systems, Palo Alto, USA), and KBP final plans, which received further re-optimization (RP_f) for CSI.

Patients and methods

Ethics statement

The Institutional Review Board of the Dalin Tzu Chi Hospital, Buddhist Tzu Chi Medical Foundation approved this study (approval number, B10804011-1) and waived the requirement for written informed consent from the patients involved because only anonymized images were retrospectively analyzed, and this study did not affect the actual treatments these patients received before.

Patients

This study retrospectively collected computed tomography (CT) image sets of 38 anonymized adults assessed between 2014 and 2019. All the image sets met the requirement of immobilization, supine position, and scan from head to pelvis. The slice thickness and matrix size were 3–5 mm and 512 × 512 voxels, respectively (Figure 1).

Target and OAR delineation

The clinical target volume (CTV) includes the whole brain and spinal cord, typically extended to the lumbar spine L3 level. Assembled CTV was

separated into CTV-brain, CTV-spine-superior, and CTV-spine-inferior for the multiple field optimization (Figure 2). The PTV-brain was constructed by symmetrically extending the CTV-brain by 3 mm and by adding 5 mm margin to the spine area. The maximum and minimum lengths of the CTV were 77.83 cm and 65.40 cm, while those of the PTV were 78.80 cm and 66.38 cm. The mean lengths of the CTV and PTV were 71.15 ± 4.28 cm and 72.23 ± 4.16 cm, respectively. The mean CTV and PTV were 1413.40 ± 162.18 cm³ and 1823.93 ± 192.14 cm³, respectively. For planning evaluation purposes, the PTV-brain, PTV-spine-superior, and PTV-spine-inferior were combined as PTV.

Dose prescription

The dose prescription was 36 Gy in 18 daily fractions. All plans were normalized so that 95% of the PTV received 100% of the prescribed dose.

Treatment planning

The 38 CT image sets of anonymized adults were imported to Eclipse TPS version 13.6 (Varian Medical Systems, Palo Alto, CA, USA). Overall, six medical physicists were participated in this study. Plans for each patient were reviewed and approved by the same physician. A TrueBeam linear accelerator (Varian Medical Systems, Palo Alto, CA, USA) equipped with a 120-leaf multileaf collimator was selected. All plans were set as 6 megavoltage for the VMAT technique. Analytical Anisotropic Algorithm dose calculation algorithm, 2.5 mm dose calculation grid, and jaw tracking were used. The mean lateral field size for the brain field is 14.76 ± 0.08 cm, while the average lateral field size for the spine field is 12.42 ± 2.52 cm. These dimensions are adjusted to encompass the entire target within a reasonable rotation range. Jaw tracking technique is used to minimize the impact of transmission leakage dose to normal organ. The collimator rotation angle is set within a range of ± 35 degrees for the head and ± 12 degrees for the spine, according to the physician's discretion at the time.

The whole target length was more than 100 cm, whereas the maximum single-field size of a linear accelerator at the isocenter is 40×40 cm. Therefore, multiple fields and three isocenters were required. The PTV-brain used two full arcs, with the isocenter positioned at the center of the brain. For the PTV-spine, two or four partial arcs were used on the PTV-spine-superior, and PTV-spine-inferior to avoid the 60–120-degree and 240–300-degree

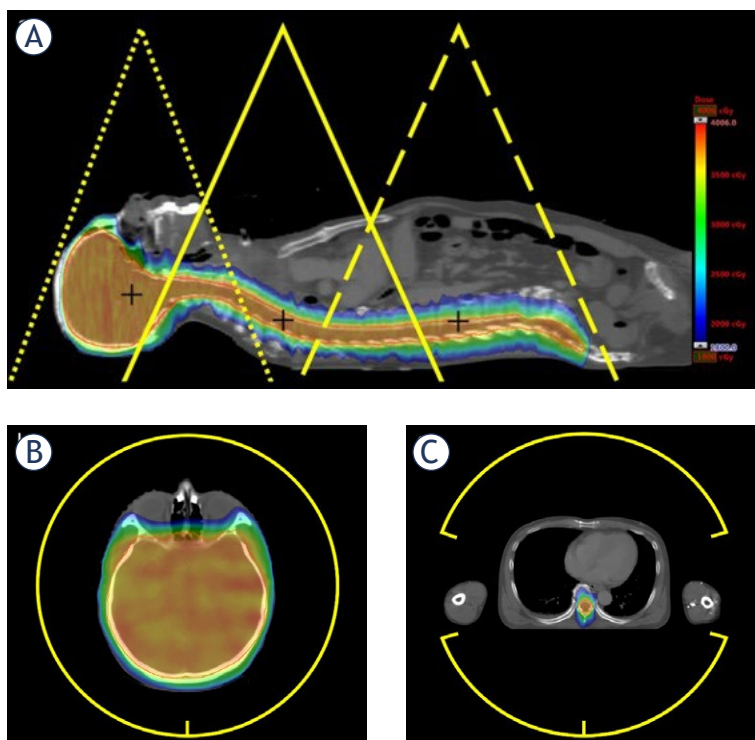


FIGURE 2. Example of the target and field setup. (A) The arrangement of the brain field (dotted lines), spine-superior field (solid lines), spine-inferior field (dashed lines), and their isocenters. Each field overlaps at least 5 cm for the low-dose gradient junction. (B) Full arc was used on the brain field. (C) Partial arc was used in the spinal fields for arm sparing.

direction for arm sparing. For the sake of clinical convenience, the three isocenters were aligned along the same X-axis (left-right). The spine isocenter shared the same X and Y coordinates, differing only along the Z-axis (craniocaudal) (Figure 2).

A total of 38 MPs were generated for the 38 patients, with 23 MPs used to train the RapidPlan (RP) model, and 15 MPs used for validation and comparison (Figure 1). Using RP, 15 RP initial plans (RP_I) were generated without manual modification, on which we performed further manual re-optimization to generate 15 RP final plans (RP_F). Finally, we compared the following three plan groups: MP, RP_I, and RP_F.

Knowledge-based planning

The RapidPlan is a commercial KBP program integrated within the Eclipse TPS. The KBP program references a library of previously clinically accepted treatment plans. It analyzes the geometric and dosimetric features, such as structure sets, field geometry, dose matrices and plan prescriptions of those plans to train a statistical model. This mod-

el is then used to predict an achievable range of DVHs and generate dose-volume objectives for a new plan.

RapidPlan algorithm

The RapidPlan algorithm comprises two main components: model configuration and DVH estimation. The model configuration component is responsible for setting up new DVH estimation models, which are subsequently utilized in the DVH estimation component to generate estimates for an individual plan. The model configuration component encompasses two distinct phases: data extraction and model training. On the other hand, the DVH estimation component encompasses the phases of estimation generation and objective generation.

The minimum requirement of data extraction and model training was 20 plans with their targets and OARs. Among the 20 randomly selected plans for model training, the right lens of three plans were too small to evaluate. Therefore, we added three more plans to meet the training requirement.

The model training phase within the DVH estimation algorithm is dedicated to the creation of DVH estimation models. The estimation generation phase calculates for each supported structure the same metrics that were calculated during the data extraction of the DVH estimation model, except for the DVH. Once the estimation generation phase has derived the upper and lower bound DVHs, the optimization objectives placement phase translates them into optimization objectives.

Plan quality, planning time, and monitor unit comparison

There were 27 dosimetric goals of irradiated fields and OARs were evaluated for the three groups among 15 patients. One patient had previously undergone thyroidectomy, and his thyroid dose could not be evaluated. This resulted in a total of 404 items being calculated for model evaluation. Dosimetric characteristics, such as V_{95} , V_{100} , V_{107} , D_{mean} , D_{max} , and D_2 of CTV, and PTV, were evaluated. In addition, conformity index (CI) and homogeneity index (HI) of the targets and dose gradient ($R_{x\%}$) were compared.¹⁴ The Radiation Therapy Oncology Group (RTOG) criteria define CI values to be between 1.0 and 2.0 in accordance with the protocol, 2.0 to 2.5 and 0.9 to 1.0 as a minor deviation, and > 2.5 and < 0.9 as a major deviation from the protocol. The CI was defined as a ratio between

the volume covered by the reference isodose (36 Gy) and the target volume, as in Equation [1].

$$CI_{RTOG} = \frac{V_{RI}}{TV} \quad [1]$$

where V_{RI} = Reference isodose volume and TV = target volume.

The HI is the ratio between maximum isodose and reference isodose. The formula of HI was shown as Equation [2]. The ideal value is 1, which increases as the plan becomes less homogeneous.

$$HI_{RTOG} = \frac{I_{max}}{RI} \quad [2]$$

Where I_{max} = maximum isodose in the target and RI = reference isodose.

The dose gradient ($R_{x\%}$) formula is given below:

$$R_{x\%} = \frac{V_{x\%}}{TV} \quad [3]$$

where $V_{x\%}$ = percentage of isodose volume, and TV = target volume.

The pre-optimization, optimization, and re-optimization planning times were compared. The pre-optimization time included OARs contouring and field setup, and the re-optimization time was the time of further optimization and calculation until the plan was satisfied. Average monitor units (MUs) were also evaluated.

Statistical analysis

The Wilcoxon test was used to compare the differences between the three groups. The differences in the dose coverage, mean dose of the targets, and OARs were compared with a 95% confidence interval. All tests were two-sided. A p value of < 0.05 was considered statistically significant. SPSS statistical package (version 17; SPSS Inc., Chicago, IL) was used for all statistical analysis.

Results

Target coverage and OAR sparing

Table 1 shows the dosimetric results of targets. For the V_{100} , V_{107} , D_{max} , and D_2 of the CTV, both MP and RP_F groups were significantly better than RP_I ($P < 0.01$). MP and RP_F in most subjects were not significantly different, except for V_{95} . For PTV, the V_{100} was normalized to 95% prescribed dose for all three groups, MP, RP_V , and RP_F . MP and RP_F groups had significantly better V_{107} , D_{max} , D_2 , and HI than did the RP_I group ($P < 0.01$). The MP group had a worse CI than the other groups. In addition, among 13 compared parameters (Table 1), the RP_I had worse results in 84.62% (11/13) parameters

TABLE 1. Dosimetric comparison between manual plans, RapidPlan initial, and RapidPlan final

Parameters	Goals	Results			P value		
		MP	RP _I	RP _F	MP vs. RP _I	MP vs. RP _F	RP _I vs. RP _F
CTV							
V ₉₅ [%]	> 99	99.99 ± 0.03	99.98 ± 0.03	99.97 ± 0.03	0.36	0.03*	0.09
V ₁₀₀ [%]	> 99	99.20 ± 0.17	98.37 ± 0.33	99.37 ± 0.23	< 0.01**	0.07	< 0.01**
V ₁₀₇ [%]	Minimize	0.62 ± 0.59	2.94 ± 4.33	0.46 ± 0.66	< 0.01**	0.16	< 0.01**
D _{mean} [Gy]	36	37.23 ± 0.18	37.31 ± 0.21	37.22 ± 0.24	0.07	0.87	0.13
D _{max} [Gy]	Minimize	39.38 ± 0.40	40.38 ± 0.57	39.42 ± 0.41	< 0.01**	0.78	< 0.01**
D ₂ [%]	< 107	106.12 ± 0.73	106.95 ± 0.96	105.72 ± 0.84	< 0.01**	0.19	< 0.01**
PTV							
V ₉₅ [%]	> 98	99.68 ± 0.15	99.55 ± 0.23	99.24 ± 0.32	0.03*	< 0.01**	< 0.01**
V ₁₀₀ [%]	= 95	95.00 ± 0.00	95.00 ± 0.00	95.00 ± 0.00	-	-	-
V ₁₀₇ [%]	Minimize	0.62 ± 0.57	3.01 ± 4.12	0.44 ± 0.61	< 0.01**	0.17	< 0.01**
D _{mean} [Gy]	36	37.10 ± 0.16	37.22 ± 0.18	37.08 ± 0.20	0.05	0.73	0.01*
D _{max} [%]	< 112	109.99 ± 1.17	112.89 ± 1.78	110.17 ± 1.14	< 0.01**	0.57	< 0.01**
D ₂ [%]	< 107	106.09 ± 0.73	107.00 ± 0.93	105.71 ± 0.80	< 0.01**	0.21	< 0.01**
CI	1	0.98 ± 0.01	1.01 ± 0.01	1.00 ± 0.01	< 0.01**	< 0.01**	0.01*
HI	1	1.10 ± 0.01	1.13 ± 0.02	1.10 ± 0.01	< 0.01**	0.57	< 0.01**

CI = conformity index; CTV = clinical target volume; Dx = minimum dose received by the hottest x% volume; HI = homogeneity index; MP = manual plan; PTV = planning target volume; RP_I = RapidPlan initial; RP_F = RapidPlan final; Vx = volume receiving at least x dose; * = P < 0.05; ** = P < 0.01

compared to the MP and RP_F groups, which had the best results in 30.77% (4/13) and 61.53% (8/13) parameters, respectively. The value of HI was the same in the MP and RP_F groups.

Furthermore, there were 14 OARs and 20 evaluation parameters for these OARs (Table 2). RP_F and RP_I had better dosimetric results than MP for the D_{mean} of optic nerves, parotid glands, heart, and esophagus, and D_{max} of eyes (all P < 0.05). The RP_F group was significantly better than the RP_I group in 11 parameters (P ≤ 0.01); no parameter in the RP_F group was worse than any parameter in the RP_I group. RP_F had comparable results to the MP group in the other OARs including, brain, brain stem, chiasma, lens, thyroid, lungs, liver, and kidneys. In conclusion, when comparing the three groups, except the heart V₄₀, which was 0% in all these three groups, the MP and RP_I groups obtained the worst results in 63.16% (12/19) and 36.84% (7/19) OAR parameters, respectively. On the contrary, the RP_F group had 73.68% (14/19) OAR parameters that were superior or equal to the other two groups.

Overall, the RP_F group achieved superior or equal best results in 71.88% (23/32) of the 32 evaluation parameters of the targets (13) and OARs (19), which excluding the PTV V_{100%} and heart V_{40Gy} because the volumes were the same in all three groups.

In this study, we evaluated the quality of the treatment plans for three groups of 15 patients each. We used 27 parameters to evaluate each plan, for a total of 404 parameters, due to one patient who did not have a thyroid gland. We did not include the parameters CTV V_{107%}, CTV D_{mean}, CTV D_{max}, PTV V_{107%}, PTV D_{mean}, CI, and HI in the evaluation because they did not have specific goal values. The plan quality pass rate of the MP and RP_F groups was 100% (404/404) according to the plan goals of targets and OARs. The RP_I group pass rate was 89.36% (361/404). When evaluating the failures of the RP_I group, although no patient in the RP_I group passed the CTV V₁₀₀ goal of 99%, the minimum and median values of RP_I CTV V₁₀₀ were 97.83% and 98.44%, respectively, and both the CTV V₉₅ and the PTV V₉₅ of RP_I group reached the goals.

TABLE 2. Dosimetric goals and results for organs at risk

OAR parameters	Goals	Results			P value		
		MP	RP _I	RP _F	MP vs. RP _I	MP vs. RP _F	RP _I vs. RP _F
Brain							
D _{max} [Gy]	< 60	39.34 ± 0.39	40.24 ± 0.61	39.28 ± 0.37	< 0.01**	0.46	< 0.01**
Brain stem							
D _{max} [Gy]	< 54	38.48 ± 0.41	39.03 ± 0.46	38.51 ± 0.28	< 0.01**	0.91	< 0.01**
Chiasm							
D _{mean} [Gy]	< 50	37.15 ± 0.35	37.10 ± 0.32	36.95 ± 0.32	0.69	0.07	0.06
D _{max} [Gy]	< 55	38.13 ± 0.40	38.73 ± 0.55	38.20 ± 0.26	0.01*	0.46	< 0.01**
Optic nerves							
D _{mean} [Gy]	< 50	27.61 ± 3.40	22.90 ± 2.39	22.42 ± 2.29	< 0.01**	< 0.01**	0.05
D _{max} [Gy]	< 55	37.13 ± 0.69	36.36 ± 1.72	36.15 ± 1.39	0.13	0.02*	0.13
Eyes							
D _{max} [Gy]	< 50	25.55 ± 3.57	22.52 ± 3.83	21.60 ± 3.86	0.02*	0.01*	0.01*
Lens							
D _{max} [Gy]	< 10	8.40 ± 0.68	8.87 ± 1.00	8.10 ± 0.55	0.11	0.21	< 0.01**
Parotid glands							
D _{mean} [Gy]	< 25	7.38 ± 2.52	5.16 ± 0.39	4.95 ± 0.39	< 0.01**	< 0.01**	< 0.01**
Spinal cord							
D _{max} [Gy]	< 50	38.93 ± 0.51	39.81 ± 0.67	39.04 ± 0.56	< 0.01**	< 0.01**	< 0.01**
Thyroid							
D _{max} [Gy]	< 45	17.23 ± 4.04	16.68 ± 2.13	16.38 ± 2.04	0.59	0.36	0.07
Lungs							
D _{mean} [Gy]	< 13	4.63 ± 0.30	4.95 ± 0.43	4.63 ± 0.24	0.03*	0.73	< 0.01**
V _{20Gy} [%]	< 22	0.06 ± 0.11	0.04 ± 0.08	0.03 ± 0.04	0.64	0.44	0.33
V _{5Gy} [%]	< 42	36.48 ± 2.88	42.77 ± 5.62	37.11 ± 2.87	0.01*	0.69	< 0.01**
Heart							
D _{mean} [Gy]	< 10	6.76 ± 1.47	5.53 ± 0.82	5.70 ± 0.93	0.01*	0.02*	0.33
V _{40Gy} [%]	< 3	0.00 ± 0.00	0.00 ± 0.00	0.00 ± 0.00	-	-	-
V _{18Gy} [%]	< 5	0.04 ± 0.10	0.01 ± 0.03	0.01 ± 0.02	0.31	0.23	0.41
Esophagus							
D _{mean} [Gy]	< 34	14.34 ± 1.62	13.23 ± 1.63	13.30 ± 1.74	0.01*	< 0.01**	0.96
Liver							
D _{mean} [Gy]	< 30	4.82 ± 0.94	4.57 ± 0.73	4.45 ± 0.70	0.61	0.33	< 0.01**
Kidneys							
D _{mean} [Gy]	< 18	2.81 ± 1.17	2.47 ± 0.46	2.38 ± 0.43	0.96	0.73	< 0.01**

OAR = organ at risk; MP = manual plan; RP_I = RapidPlan initial; RP_F = RapidPlan final; V_x = volume receiving at least x dose; * = P < 0.05; ** = P < 0.01

TABLE 3. The mean dose of the OARs outside the targets contours

Organ	Mean dose			P value		
	MP	RP _I	RP _F	MP vs. RP _I	MP vs. RP _F	RP _I vs. RP _F
Optic nerves	27.61 ± 3.40	22.90 ± 2.39	22.42 ± 2.29	< 0.01**	< 0.01**	0.05
Eyes	12.11 ± 1.99	10.16 ± 0.55	9.83 ± 0.74	0.01*	0.01*	0.02*
Lens	7.09 ± 0.67	7.21 ± 0.52	6.78 ± 0.39	0.43	0.16	< 0.01**
Parotid glands	7.38 ± 2.52	5.16 ± 0.39	4.95 ± 0.39	< 0.01**	< 0.01**	< 0.01**
Thyroid	10.41 ± 3.37	9.00 ± 1.94	8.51 ± 2.07	0.06	0.04*	< 0.01**
Lungs	4.63 ± 0.30	4.95 ± 0.43	4.63 ± 0.24	0.03*	0.73	< 0.01**
Heart	6.76 ± 1.47	5.53 ± 0.82	5.70 ± 0.93	0.01*	0.02*	0.33
Liver	4.82 ± 0.94	4.57 ± 0.73	4.45 ± 0.70	0.61	0.33	< 0.01**
Kidneys	2.81 ± 1.17	2.47 ± 0.46	2.38 ± 0.43	0.96	0.73	< 0.01**

Bold type = the highest D_{mean} in the three groups; MP = manual plan; RP_I = RapidPlan initial; RP_F = RapidPlan final; Underline mark = the lowest D_{mean} in the three groups; * = $P < 0.05$; ** = $P < 0.01$

The pass rates of CTV $D_{2\%}$, PTV D_{max} , and PTV $D_{2\%}$ for the RP_I group, were 66.67% (10/15), 33.33% (5/15), and 66.67% (10/15), respectively. In addition, in the OAR, the lens D_{max} and lungs V_5 of the RP_I group did not meet the goals. The pass rate of the lens D_{max} was 93.33% (14/15) for the RP_I group. In one RP_I plan, the lens D_{max} was 10.98 Gy > 10 Gy. Lastly, the RP_I lungs V_5 pass rate was 53.33% (8/15).

Table 3 shows the mean dose of the 9 OARs. The highest OARs D_{mean} of the optic nerves, eyes, parotid glands, thyroid, heart, liver, and kidneys; and lens and lungs in these three groups were obtained in the MP group (78%, 7/9) and RP_I group (22%, 2/9), respectively. The lowest OARs D_{mean} were mostly in the RP_F group (89%, 8/9). Comparing RP_I and MP, RP_F and RP_I, and RP_F and MP groups, the RP_I group significantly reduced the doses of optic nerves, eyes, parotid glands, and heart than the MP group; the RP_F group further significantly reduced the doses of eyes, lenses, parotid glands, thyroid, lungs, liver, and kidneys than the RP_I group ($P \leq 0.05$); and RP_F significantly reduced the doses of optic nerves, eyes, parotid glands, thyroid, and heart, respectively than the MP group ($P < 0.05$).

In the low-dose region of normal tissue, we employed $R_{50\%}$, $R_{30\%}$, and $R_{10\%}$ as dose gradient indicators. The values for MP, RP_I, and RP_F at $R_{50\%}$ were 2.27 ± 0.13 , 2.26 ± 0.16 , and 2.26 ± 0.14 , respectively. For $R_{30\%}$, the values were 3.96 ± 0.31 , 3.95 ± 0.32 , and 3.94 ± 0.37 , respectively. The corresponding values for $R_{10\%}$ were 10.15 ± 1.93 , 10.08 ± 1.69 , and 10.00 ± 1.74 . There were no statistically significant differences among the three groups ($P > 0.05$).

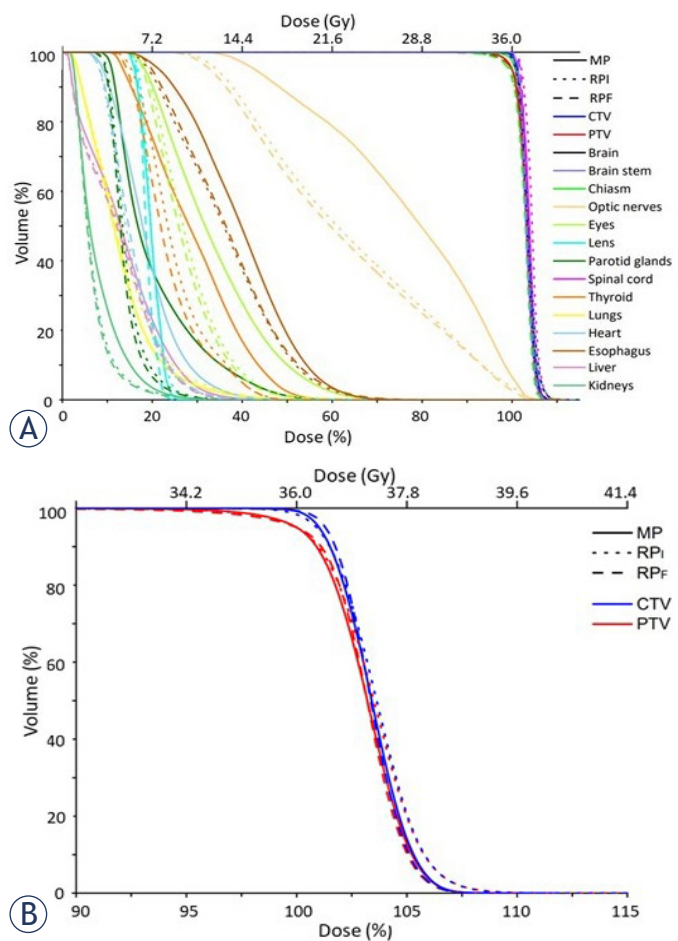


FIGURE 3. (A) Population-averaged dose-volume histogram (DVH) for all organs at risk and targets. (B) The population-averaged DVH for targets only.

CTV = clinical target volume; MP = manual optimization plan; PTV = planning target volumes; RP_I = RapidPlan initial; RP_F = final RapidPlan after manual re-optimization

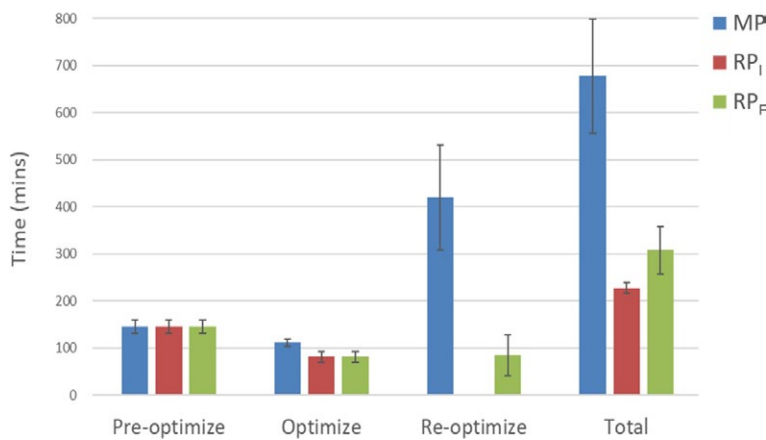


FIGURE 4. Comparison of the planning time for MP, RP_I, and RP_F. The error bar represents one standard deviation.

MP = manual optimization plan; RP_I = RapidPlan initial; RP_F = final RapidPlan after manual re-optimization

Figure 3A showed the population-averaged DVH of targets and OARs. In the DVH, the doses of optic nerves, eyes, lens, parotid glands, thyroid, liver, and kidneys in RP_F or RP_I were lower than those in MP. Furthermore, the DVH of RP_F OARs was better than those of RP_I OARs. Figure 3B shows the targets coverage of CTV and PTV. In the shoulder part of the DVH, with the 95% volume of targets, the MP and RP_I groups had the same targets coverage, while the RP_F group had a slightly better 95% volume dose coverage than the other two groups. The DVH tail part, the high dose in 5% volume, showed that the RP_I had the highest dose in the craniospinal area. The population-averaged DVH showed that the RP_F group had the best targets coverage, homogenous targets dose distribution, and OAR dose avoidance among these three groups.

Treatment planning time

The pre-optimization time was the same in all three groups (146 minutes, Figure 4). The optimization process took a significantly longer time in the MP group than in the RP_I and RP_F groups with 111.45, 81.68, and 81.68 minutes ($P < 0.05$), respectively. The re-optimization time in the MP was significantly longer than in the RP_F group (420.36 versus 85.13 minutes, $P < 0.05$). There was no re-optimization in the RP_I group. Overall, the entire planning time was longer in the MP group than in

the RP_I (677.80 versus 227.66 minutes, $P < 0.05$) and RP_F (677.80 versus 307.76 minutes, $P < 0.05$) groups. The total planning time-saving rates (saved planning time) of RP_I and RP_F were 66.41% (450.14 minutes) and 54.59% (370.04 minutes), respectively, compared to the MP group.

MU comparison

The average MU values with one standard deviation of MP, RP_I, and RP_F groups were 935.24 ± 128.44 , 1013.22 ± 114.92 , and 1026.46 ± 149.43 , respectively, with no significant difference between these three groups (all $P > 0.05$).

Discussion

Our research discovered that by utilizing 23 plans to develop the KBP model in combination with RP and re-optimization in CSI, we were able to significantly shorten the planning time by half and enhance plan quality.

Incorporating more patients in the model libraries for model training have a possibility to lead to fewer outliers and more consistent plan quality.¹⁵⁻¹⁷ However, the application of the CSI technique in clinical practice is not common in most hospitals. In this study, because CSI treatment is relatively rare, we searched databases covering the previous 6 years and found only 38 CT image sets. The Varian accelerator company recommended a minimum of 20 to 25 treatment plans in training set for a specific target. According to the study by Jim P. Tol *et al.*¹⁸, Increasing the number of plans used in model training was found to produce comparable results. Based on recommendations, previous experience, and the limited availability of clinical CSI cases, we used 23 plans to complete the model training and compared them with 15 manual plans.

The traditional CSI used patient prone position to reduce the OARs radiation dose via simple two lateral opposed and posterior-anterior (PA) fields. However, this technique can create dose non-uniform in the field junction area. The commonly encountered pediatric CSI typically requires two fields and one junction to achieve coverage. This study aims to validate whether KBP can perform effectively in more complex scenarios, utilizing adult CSI as a test case. We used the VMAT technique to disperse the radiation dose in OARs and enhance the homogeneity of the targets dose. The VMAT technique delivers radiation from all angles, which causes it to be attenuated as it passes

through the couch. Our medical physicist compensated for this effect by calculating the attenuation of the couch.¹⁹ Furthermore, cone beam computed tomography ensured an accurate treatment location. Therefore, in this study, all treatment plans were designed using the supine position, which could make patients more comfortable, relaxed, and stable during treatment.^{3,20}

Although the plan parameter pass rate of RP_I was only 89.36%, the RP_I target coverage of minimum CTV V₉₅ and PTV V₉₅ values were $\geq 99.90\%$ and $\geq 99.00\%$, respectively, which were both higher than 95%, the clinical common plan acceptable criteria.²¹ Compared with the traditional 3D-CRT technique, by which the high dose area might receive approximately twice the prescribed dose at the field overlapping sites, the highest PTV D_{max} in RP_I was 115.57% which was much lower than the traditional 3D-CRT technique. For OARs, all 14 plans in RP_I achieved the goal (< 10 Gy) except for one plan with lens D_{max} 10.98 Gy, which did not reach the goal. Table 2 shows that the heart D_{mean} in RP_I was also the lowest of the three groups. Although, Uehara *et al.* reported that KBP was found clinically unacceptable after a single optimization without manual objective constraints in head and neck cancer.²² Most studies in the other body sites, such as gynecological, prostate, and rectal cancers, support that the RP plan would be comparable to the manual plan.²³ In our study, the RP_I plans were clinically acceptable for CSI and approved by the physician.

The DVH distribution is one of the vital plan evaluation tools. The DVH of OARs (Figure 3) showed that most of the OARs in the MP group received higher doses than RP_I and RP_F as shown by the D_{mean} and D_{max} in Table 2. In the target DVH (Figure 3B), the RP_F group had better 95% volume dose coverage and better performance at reducing high doses than the other two groups. According to our CI results, there was a minor deviation of the target in the MP group; however, RP_I or RP_F could have achieved the planning goal. Furthermore, HI values in this study show that MP and RP_F groups had better homogeneity than did RP_I. Previous studies on lung cancer or prostate cancer showed that KBP could reduce the OARs dose²³; however, target coverage and dose homogeneity of KBP did not always have better results than the manual plan. Our study on CSI showed that RP improved the plan quality of OARs and that additional re-optimization after initial RP could improve the plan quality, as previous studies showed in other cancer sites.²⁴⁻²⁷

In terms of cardiac doses, all three plans (MP, RP_I, and RP_F) exhibited notably low V_{40Gy} and V_{18Gy} values, comfortably below the established cardiac dose constraints. It is pertinent to mention that the mean cardiac dose for RP_I was already lower than that for MP. Therefore, the primary focus during the optimization process was not predominantly on further reducing cardiac dose. In the case of RP_I, the lungs V_{5Gy} value ($42.77 \pm 5.62\%$) surpassed the target threshold of 42%. Subsequently, in the ensuing RP_F optimization, concerted efforts were undertaken to amplify the reduction of lungs V_{5Gy} values, resulting in a dose shift towards the heart. Nevertheless, from a statistical perspective, the P-value for the comparison between RP_I and RP_F exceeded 0.05.

In our study, RP_I and RP_F reduced planning time compared to MP by 66.41% (450.14 minutes) and 54.59% (370.04 minutes), respectively. The result showed that KBP for CSI might save more planning time in complex plans with many OARs than in general cancer sites. Previously, Wells *et al.*²⁸ reported that KBP could reduce planning time by approximately 30 minutes per breast cancer patient. Visak *et al.*²⁹ reported that all the RP plans required less than 30 minutes of planning time for lung cancer. Masi *et al.*³⁰ showed that the time required for the production of the KBP plan was 6–15 minutes, compared to manual planning requiring 30–150 minutes for a commercial TPS and 15–60 minutes after 8 months of commercial TPS usage in prostate cancer. Furthermore, Chatterjee *et al.*³¹ showed that the KBP planning time for the multi-form brain glioblastoma was typically 13 minutes for VMAT, compared to the typical 4 hours for the manual planning method. Amaloo *et al.*³² showed that the total planning time was reduced from 120 minutes to 20 minutes in prostate cancer patients. In a study of nasopharyngeal cancer, Chang *et al.*³³ concluded that the total RP planning time is only about one-fifth that of MP. Similarly, our KBP study for CSI, a very long treatment size from the brain to the lumbosacral area, could effectively reduce the planning time while improving the plan quality, as shown in previous KBP studies for other cancer sites.

Conclusions

This study used 23 plans to train the KBP CSI model and investigated the difference between MP and RP for the same patients and found that RP plans after re-optimization could halve the planning

time and improve plan quality. According to our study result, medical physicists at low CSI patient volume hospitals could efficiently produce CSI plans by the KBP method.

Acknowledgements

We would like to thank Ms. Feng-Chun Hsu for statistical support, Dr. Liang-Cheng Chen for his advice for clinical aspects of this project. This study was supported by research grants from the Dalin Tzu Chi Hospital (grant number: DTCRD109-I-18). The funders had no role in the study design, data collection and analysis, decision to publish, or the preparation of the manuscript.

References

- Seidel C, Heider S, Hau P, Glasow A, Dietzsch S, Kortmann RD. Radiotherapy in medulloblastoma-evolution of treatment, current concepts and future perspectives. *Cancers* 2021; **13**: 5945. doi: 10.3390/cancers13235945
- Kiltie AE, Povall JM, Taylor RE. The need for the moving junction in craniospinal irradiation. *Br J Radiol* 2000; **73**: 650-4. doi: 10.1259/bjr.73.870.10911789
- Mani KR, Sapru S, Maria Das KJ, Basu A. A supine cranio-spinal irradiation technique using moving field junctions. *Pol J Med Phys Eng* 2016; **22**: 79-83. doi: 10.1515/pjmpe-2016-0014
- Mancosu P, Cozzi L, Muren LP. Total marrow irradiation for hematopoietic malignancies using volumetric modulated arc therapy: a review of treatment planning studies. *Phys Imaging Radiat Oncol* 2019; **11**: 47-53. doi: 10.1016/j.phro.2019.08.001
- Seravalli E, Bosman M, Lassen-Ramshad Y, Vestergaard A, Oldenburger F, Visser J, et al. Dosimetric comparison of five different techniques for craniospinal irradiation across 15 European centers: analysis on behalf of the SIOP-E-BTG (radiotherapy working group). *Acta Oncol* 2018; **57**: 1240-9. doi: 10.1080/0284186X.2018.1465588
- Prabhu RS, Dhakal R, Piantino M, Bahar N, Meaders KS, Fasola CE, et al. Volumetric modulated arc therapy (VMAT) craniospinal irradiation (CSI) for children and adults: a practical guide for implementation. *Pract Radiat Oncol* 2022; **12**: e101-e9. doi: 10.1016/j.proro.2021.11.005
- Sarkar B, Pradhan A. Choice of appropriate beam model and gantry rotational angle for low-dose gradient-based craniospinal irradiation using volumetric-modulated arc therapy. *J Radiother Pract* 2016; **16**: 53-64. doi: 10.1017/s146039691600042x
- Sarkar B, Munshi A, Manikandan A, Roy S, Ganesh T, Mohanti BK, et al. A low gradient junction technique of craniospinal irradiation using volumetric-modulated arc therapy and its advantages over the conventional therapy. *Cancer Radiother* 2018; **22**: 62-72. doi: 10.1016/j.canrad.2017.07.047
- Hussein M, Heijmen BJM, Verellen D, Nisbet A. Automation in intensity modulated radiotherapy treatment planning-a review of recent innovations. *Br J Radiol* 2018; **91**: 20180270. doi: 10.1259/bjr.20180270
- Ma C, Huang F. Assessment of a knowledge-based RapidPlan model for patients with postoperative cervical cancer. *Prec Radiat Oncol* 2017; **1**: 102-7. doi: 10.1002/pro6.23
- Fogliata A, Reggiori G, Stravato A, Lobefalo F, Franzese C, Franceschini D, et al. RapidPlan head and neck model: the objectives and possible clinical benefit. *Radiat Oncol* 2017; **12**: 73. doi: 10.1186/s13014-017-0808-x
- Hu J, Liu B, Xie W, Zhu J, Yu X, Gu H, et al. Quantitative comparison of knowledge-based and manual intensity modulated radiation therapy planning for nasopharyngeal carcinoma. *Front Oncol* 2020; **10**: 551763. doi: 10.3389/fonc.2020.551763
- Castriconi R, Fiorino C, Passoni P, Broggi S, Di Muzio NG, Cattaneo GM, et al. Knowledge-based automatic optimization of adaptive early-regression-guided VMAT for rectal cancer. *Phys Med* 2020; **70**: 58-64. doi: 10.1016/j.ejmp.2020.01.016
- Shaw E, Kline R, Gillin M, Souhami L, Hirschfeld A, Dinapoli R, et al. Radiation Therapy Oncology Group: radiosurgery quality assurance guidelines. *Int J Radiat Oncol Biol Phys* 1993; **27**: 1231-9. doi: 10.1016/0360-3016(93)90548-a
- Boutillier JJ, Craig T, Sharpe MB, Chan TC. Sample size requirements for knowledge-based treatment planning. *Med Phys* 2016; **43**: 1212-21. doi: 10.1118/1.4941363
- Cagni E, Botti A, Wang Y, Iori M, Petit SF, Heijmen BJM. Pareto-optimal plans as ground truth for validation of a commercial system for knowledge-based DVH-prediction. *Phys Med* 2018; **55**: 98-106. doi: 10.1016/j.ejmp.2018.11.002
- Wang M, Gu H, Hu J, Liang J, Xu S, Qi Z. Evaluation of a highly refined prediction model in knowledge-based volumetric modulated arc therapy planning for cervical cancer. *Radiat Oncol* 2021; **16**: 58. doi: 10.1186/s13014-021-01783-9
- Tol JP, Delaney AR, Dahele M, Slotman BJ, Verbakel WF. Evaluation of a knowledge-based planning solution for head and neck cancer. *Int J Radiat Oncol Biol Phys* 2015; **91**: 612-20. doi: 10.1016/j.ijrobp.2014.11.014
- Yu CY, Chou WT, Liao YJ, Lee JH, Liang JA, Hsu SM. Impact of radiation attenuation by a carbon fiber couch on patient dose verification. *Sci Rep* 2017; **7**: 43336. doi: 10.1038/srep43336
- Sarkar B, Munshi A, Ganesh T, Manikandan A, Mohanti BK. Dosimetric comparison of short and full arc in spinal PTV in volumetric-modulated arc therapy-based craniospinal irradiation. *Med Dosim* 2020; **45**: 1-6. doi: 10.1016/j.meddos.2019.03.003
- Dietzsch S, Braesigk A, Seidel C, Remmele J, Kitzing R, Schlender T, et al. Pretreatment central quality control for craniospinal irradiation in non-metastatic medulloblastoma: first experiences of the German radiotherapy quality control panel in the SIOP PNET5 MB trial. *Strahlenther Onkol* 2021; **197**: 674-82. doi: 10.1007/s00066-020-01707-8
- Uehara T, Monzen H, Tamura M, Ishikawa K, Doi H, Nishimura Y. Dose-volume histogram analysis and clinical evaluation of knowledge-based plans with manual objective constraints for pharyngeal cancer. *J Radiat Res* 2020; **61**: 499-505. doi: 10.1093/jrr/rraa021
- Ge Y, Wu QJ. Knowledge-based planning for intensity-modulated radiation therapy: a review of data-driven approaches. *Med Phys* 2019; **46**: 2760-75. doi: 10.1002/mp.13526
- Wu H, Jiang F, Yue H, Zhang H, Wang K, Zhang Y. Applying a RapidPlan model trained on a technique and orientation to another: a feasibility and dosimetric evaluation. *Radiat Oncol* 2016; **11**: 108. doi: 10.1186/s13014-016-0684-9
- Castriconi R, Fiorino C, Broggi S, Cozzarini C, Di Muzio N, Calandrino R, et al. Comprehensive Intra-Institution stepping validation of knowledge-based models for automatic plan optimization. *Phys Med* 2019; **57**: 231-7. doi: 10.1016/j.ejmp.2018.12.002
- Kamima T, Ueda Y, Fukunaga JI, Shimizu Y, Tamura M, Ishikawa K, et al. Multi-institutional evaluation of knowledge-based planning performance of volumetric modulated arc therapy (VMAT) for head and neck cancer. *Phys Med* 2019; **64**: 174-81. doi: 10.1016/j.ejmp.2019.07.004
- Fogliata A, Cozzi L, Reggiori G, Stravato A, Lobefalo F, Franzese C, et al. RapidPlan knowledge based planning: iterative learning process and model ability to steer planning strategies. *Radiat Oncol* 2019; **14**: 187. doi: 10.1186/s13014-019-1403-0
- Wells DM, Walrath D, Craighead PS. Improvement in tangential breast planning efficiency using a knowledge-based expert system. *Med Dosim* 2000; **25**: 133-8. doi: 10.1016/s0958-3947(00)00039-x
- Visak J, McGarry RC, Randall ME, Pokhrel D. Development and clinical validation of a robust knowledge-based planning model for stereotactic body radiotherapy treatment of centrally located lung tumors. *J Appl Clin Med Phys* 2021; **22**: 146-55. doi: 10.1002/acm2.13120
- Masi K, Archer P, Jackson W, Sun Y, Schipper M, Hamstra D, et al. Knowledge-based treatment planning and its potential role in the transition between treatment planning systems. *Med Dosim* 2018; **43**: 251-7. doi: 10.1016/j.meddos.2017.10.001

31. Chatterjee A, Serban M, Abdulkarim B, Panet-Raymond V, Souhami L, Shenouda G, et al. Performance of knowledge-based radiation therapy planning for the glioblastoma disease site. *Int J Radiat Oncol Biol Phys* 2017; **99**: 1021-8. doi: 10.1016/j.ijrobp.2017.07.012
32. Amaloo C, Hayes L, Manning M, Liu H, Wiant D. Can automated treatment plans gain traction in the clinic? *J Appl Clin Med Phys* 2019; **20**: 29-35. doi: 10.1002/acm2.12674
33. Chang ATY, Hung AWM, Cheung FWK, Lee MCH, Chan OSH, Philips H, et al. Comparison of planning quality and efficiency between conventional and knowledge-based algorithms in nasopharyngeal cancer patients using intensity modulated radiation therapy. *Int J Radiat Oncol Biol Phys* 2016; **95**: 981-90. doi: 10.1016/j.ijrobp.2016.02.017